An integrated solar desalination with evacuated tube heat pipe solar collector and new wind ventilator external condenser

Shahin Shoeibi [a], Hadi Kargarsharifabad [a,*], Nader Rahbar [a], Gholamreza Khosravi [a], Mohsen Sharifpur [b,c,d,*]

[a] Energy and Sustainable Development Research Center, Semnan Branch, Islamic Azad University, Semnan, Iran
[b] Clean Energy Research Group, Department of Mechanical and Aeronautical Engineering, Engineering III, University of Pretoria, Lynnwood Road, Pretoria 0002, South Africa
[c] Department of Medical Research, China Medical University Hospital, China Medical University, Taichung 404, Taiwan
[d] Department of Mechanical Engineering, University of Science and Culture, Tehran, Iran

ARTICLE INFO

Keywords:
Solar desalination
Evacuated tube heat pipe
Wind ventilator
Water cooling
Environmental analysis

ABSTRACT

Over the recent decades, many investigations have been performed to enhance the performance of solar desalination. Some of these studies improved the saline water temperature, while others decreased the glass cover temperature. This study has investigated single-slope solar still using an evacuated tube heat pipe solar collector (ETHP-SC) and a new design of external condenser. The ETHP-SC increased the saline water temperature. On the other hand, the external condenser enhanced the condensation rate using a wind ventilator and a water cooling system. The pressure inside the modified solar desalination decreased by the suction of water vapor with the wind ventilator. The water vapor flowed to the external condenser and was distilled by hitting the perforated copper plate connected to the water cooling system. Results revealed that the freshwater generation of solar desalination using an external condenser and ETHP was about 2.13 times those of conventional ones. The yield fraction of the external condenser was about 18.62% of the total water productivity. Moreover, the carbon dioxide mitigation was almost 29.19 tons and 0.51 tons based on environmental and exergoenvironmental analysis in the modified solar desalination, respectively.

Introduction

The importance of fresh water in human life and civilization is not unknown. Access to pure and drinkable freshwater is the main topic in most developing countries. So far, various methods have been developed to separate salts from saline water and produce freshwater, most of which require energy generated by fossil fuels to obtain fresh water. The main problem in such systems is the environmental pollution and depletion of these energy sources. Solar energy is among the significant sources of renewable energy with many applications [1]. The use of solar energy is increasing in various fields, especially the desalination of brackish water [2]. The use of solar still has many benefits, including low maintenance and operation costs and no need to use fossil fuels. In recent years, various research has been pursued on increasing the efficiency of solar still given the low water productivity [3,4]. Changes in various parameters, including configuration [5,6], material absorption [7,8], water height [9,10], glass cover [11,12] and insulation material and thickness [13,14] improve the performance of solar desalination. Solar desalination is classified as active and passive types in terms of application. In passive solar desalination, solar energy is the only term of energy, increasing the saline water temperature and producing pure water [15]. Meanwhile, for active solar still, different techniques that raise the water temperature, including solar collector [16], phase change material [17,18], nanoparticles [19,20], thermoelectric heating [21,22], electrical heater [23], air heater [24], and photovoltaic/thermal technology [25] have been studied. Given the high water productivity and energy efficiency of active solar desalination, numerous studies have been performed on it.

An evacuated tube heat pipe solar collector (ETHP-SC) is a device for heat transfer based on thermal conductivity between solar collector and water to increase the water temperature [26]. Bhargva and Yadav [27]

* Corresponding authors at: Energy and Sustainable Development Research Center, Semnan Branch, Islamic Azad University, Semnan, Iran (H. Kargarsharifabad), Clean Energy Research Group, Department of Mechanical and Aeronautical Engineering, Engineering III, University of Pretoria, Lynnwood Road, Pretoria 0002, South Africa (M. Sharifpur).
E-mail addresses: h.kargar@semnaniau.ac.ir (H. Kargarsharifabad), mohsen.sharifpur@up.ac.za (M. Sharifpur).

Nomenclature

A_b	Surface area (m^2)
AMC	Annual maintenance operational price ($)
ASV	Annual salvage value ($)
a	Accuracy of the instrument
BCR	Benefit cost ratio
CPL	Water output cost ($ L^{-1})
CRF	Capital recovery factor
E_{in}	Embodied energy (kWh)
$(E_{en})out$	Annual energy output (kWh)
$(E_{ex})out$	Annual exergy output (kWh)
EPBT	Energy payback time (years)
EPF	Energy production factor
ETHP-SC	evacuated tube heat pipe solar collector
FAC	Fixed annual price ($)
h_{fg}	Latent heat (KJ/Kg)
i	Interest rate (%)
I_t	Solar intensity (W/m2)
$\dot{m}$	water production rate (L/s)
M	Annual productivity (L/m^2.year)
n	Lifetime (years)
P	Capital price ($)
POW	Price of water ($)
S	Salvage value ($)
SFF	Sinking fund factor
T	Temperature (℃)
u	The standard uncertainty
$\dot{W}$	Electrical equipment (W)
UAB	present worth of benefit ($)
UAC	Uniform annual cost ($)
X_{co_2}	Environmental parameter (ton CO_2)
X_{ex,co_2}	Exergoenvironmental parameter (ton CO_2)
z_{co_2}	Price of carbon ($)

Greek symbols

η_{daily}	Daily efficiency

Subscripts

a	Ambient
ev	Evaporative
ex	Exergy
s	Solar
w	Water

studied the impact of glass shading and an evacuated tube collector on the performance of solar desalination. In another study, they [28] investigated the enhanced water generation of solar desalination using a solar collector coupled with a heat exchanger, mirrors, and an external condenser. The internal mirrors were used to enhance the solar intensity of the basin liner. The results indicated increased water production rates in internal mirrors, external condenser, and evacuated tube solar desalination. Feilizadeh et al. [29] increased the water productivity of a solar desalination using a V-shape external condenser and a solar collector. They reported that the freshwater generation of new solar stills increased. Dawood et al. [30] studied the effect of solar collector and phase change material on the water output of solar desalination. Their results showed that the CPL of solar desalination using modification and traditional solar desalination were equal to 0.0154 and 0.0219 $/L, respectively. Fallahzadeh et al. [31] studied the daily yield of a pyramid solar desalination using various operating fluid solar collector. They revealed that the freshwater yield of solar desalination using a heat pipe solar collector and conventional solar desalination was equal to 6970 cc/m^2.day and 3300 cc/m^2.day, respectively. Singh et al. [32] integrated two different configurations of solar desalination with solar collector, which enhanced the water temperature and resulted in different temperatures between glass and water. The CPL of modified double slope solar desalination using solar collector declined about 15.19% in comparison with the single slope solar desalination using solar collector. They also found that the optimum water flow rate and number of evacuated tubes in both solar stills were 0.016 kg/s and 12, respectively.

Water vapor is separated from the water and flows over the glass cover due to the natural convection heat transfer between condensation and evaporation zones. The water output can increase by reducing the condensation surface temperature using the external condenser method. Simultaneous use of nanotechnology and external condenser methods has a high impact on the solar still performance. Eltawil et al. [33] studied the effect of using solar air and water heaters and an external condenser on the water generation of a solar still. Their results revealed that the daily yield of the system was improved by 51% and 82%, respectively. Kabeel et al. [34] studied the water output of solar desalination using an aluminum oxide nanofluid and an external condenser. They found that the water output of solar desalination with external condenser enhanced by 53.2%, while the external condenser and aluminum oxide nanofluid increased it by about 116% compared to conventional ones. In another study, Kabeel et al. [35] evaluated a numerical and experimental study on the impact of Al_2O_3 and Cu_2O nanofluids with external condensers on the freshwater generation of solar desalination. They revealed that the water production rate in solar desalination by Al_2O_3 and Cu_2O nanofluids and external condenser improved by 126% and 134%, respectively. Omara et al. [36] increased the water generation of corrugate wick solar desalination using aluminum oxide, cuprous nanofluids, and an external condenser. Hassan et al. [37] modified the solar desalination and compared it with conventional ones. They reported that the freshwater yield of solar desalination with parabolic trough collector and finned external condenser enhanced by 67% and 7.3 %, respectively, compared to traditional ones in the summer. Bhardwaj et al. [38] enhanced the condensation zone and used wire cable to rise the productivity of the solar desalination. According to the results, by increasing the condensation zone 7.5-fold, the water production rate inside the lab and exposed to sunlight improved by 65% and 50%, respectively.

Motivation for research

The temperature difference between condensation and evaporation area is a significant parameter in the performance of solar desalination. In this study, the ETHP-SC and a new design of external condenser were coupled with single-slope solar desalination to improve the water production rate. Water stream flowed between the manifold of ETHP-SC and saline water and increased the evaporation rate. A wind ventilator was used to reduce the pressure in the enclosure of solar desalination using wind velocity and leading water vapor to contact the water cooling system. To the best of our knowledge, the combination of a wind ventilator and a water cooling system has not been used so far to increase the condensation rate as an external condenser. Furthermore, by using ETHP-SC and a new design of external condenser with wind ventilator, the energy matrices were calculated, and environmental analysis was performed to evaluate the solar still performance.

Experimental procedure

In order to fabricate solar desalination, some important factors, such as low weight, long lifetime, corrosion, and fracture resistance, must be considered. Moreover, the enclosure of a solar still should be completely

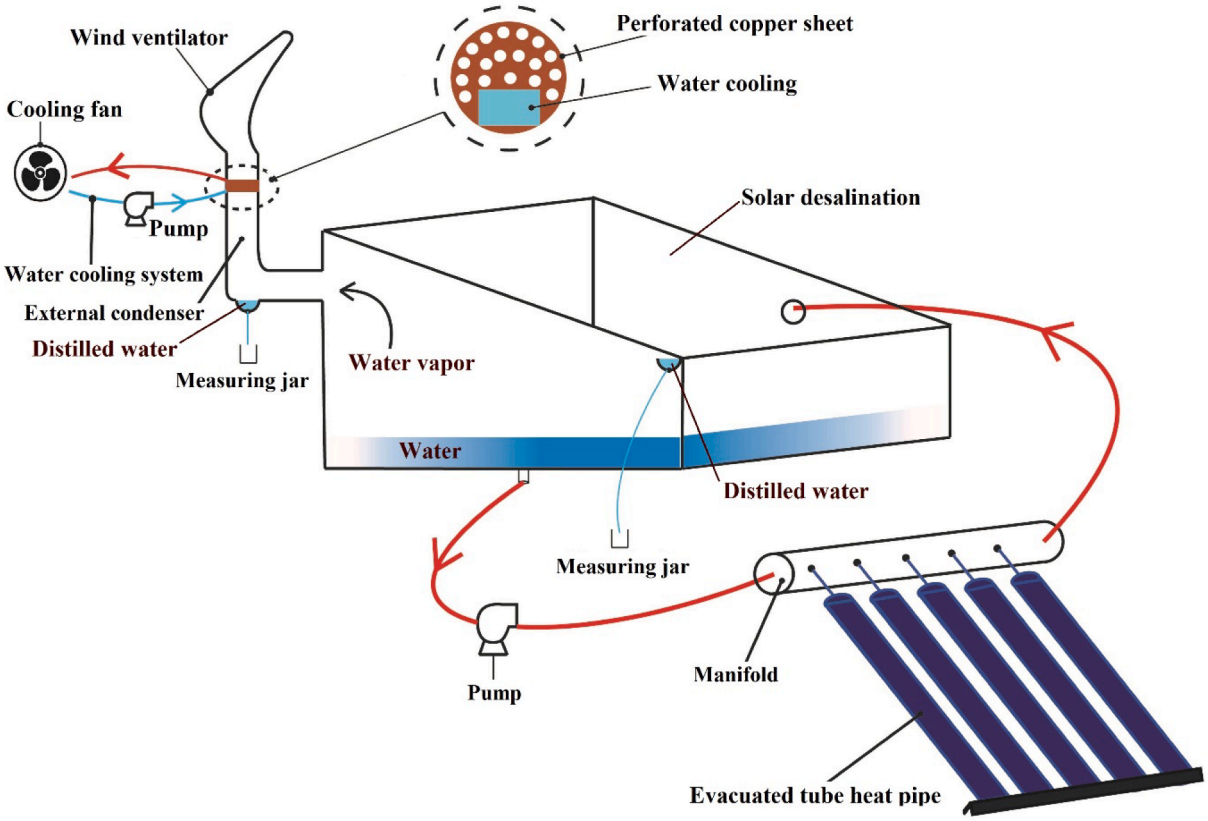

Fig. 1. Sketch view of solar desalination with ETHP-SC and external condenser (wind ventilator and water cooling system).

sealed to prevent water vapor from escaping and well insulated to decrease the heat transfer from the pool to the surrounding environment. In this study, modified and conventional solar stills with the same dimensions were tested. The electrical equipment of the modified solar still included hot water pumps in the ETHP-SC manifold and cold water pumps in the water cooling system and cooling fan, which worked with a 12 Volt DC power supply. The solar still was made of galvanized plates with a thickness of 0.006 m and basin dimensions of 0.25 m^2. The outer surface of the absorber plate was insulated with 0.03-m thick polyurethane foam, and to drain the distilled water, a gutter was welded with a low slope, which was connected to an outlet pipe to collect the generated water. In order to raise the absorption of solar intensity, the basin of the solar desalination and the walls were colored black. The glass had a thickness of 0.003 m. In order for better flows of the generated water of solar still and higher absorption of solar radiation, the angles of both glass cover and ETHP-SC were equal to 35°. An iron manifold with a diameter of 0.05 m with five holes was used for the ETHP-SC header, which was connected to condensers of five heat pipes. The hot water circulated between the saline water and the manifold through a pump with a power of 2.4 W. The hot water transmission hoses were made by PVC to decrease the heat loss. The electrical power of the hot water and cold water pumps and the cooling fan was provided by a photovoltaic panel with dimensions of 0.1 m^2. The manifold and outer surface of the basin liner were insulated with 0.04 m thickness fiberglass. The outer diameter of the evacuated tube was 0.07 m with a wall thickness of 0.002 m and a length of 1.7 m. The water was used as an operating fluid in heat pipes. The water (heat transfer medium) temperature inside the evacuated tube rose and flowed upwards into the manifold. The operating fluid of the heat pipe was constantly flowing due to the principles of thermosiphon [39]. Fig. 1 indicates the schematic of solar desalination using ETHP-SC and an external condenser.

The external condenser was used to rise the condensation rate and freshwater yield of the solar desalination. It consisted of a wind ventilator and a water cooling system. The wind ventilator was used to create a relative vacuum in the enclosure of the solar still. In fact, the vacuum in this device was created by the ambient wind, and therefore, there was no need for electrical power to produce vacuum by an electrical device, such as a fan or a pump. The wind velocity on the wind ventilator caused negative pressure in the outlet of the wind ventilator, and due to the connection to the enclosure of the solar still, it caused suction and reduced the pressure in the solar desalination. The reduction in the pressure in the solar desalination reduced the saturation temperature and increased the water vapor. Therefore, the outlet water vapor flowed to the external condenser and increased the water output of solar desalination. One end of the external condenser was connected to the top of the back wall of the solar still with a diameter of 0.05 m, and the other end was mounted to the wind ventilator with a diameter of 0.1 m. The pipe of the external condenser was made of PVC, and it had a reducer to decrease the velocity of water vapor inside the external condenser. The suction created by the wind ventilator caused a portion of the water vapor in the solar desalination to flow into the external condenser. Fig. 2 demonstrates the solar desalination with ETHP-SC and an external condenser.

In order to increase distillation and prevent water vapor loss, a perforated copper sheet connected to the water cooling was placed inside the external condenser. The water cooling acted like a heat exchanger and created a cooling zone in the water vapor path. As water vapor passed through this zone, it was distilled and collected in the lower part of the external condenser. On the copper sheet, 18 holes, 0.01 m in diameter, were punched. The water cooling system consisted of a closed loop with water (operating fluid) circulating by a pump with a power of 2 W. The copper heat sink was used for the cooling part and attached to the copper sheet to reduce its temperature. In this case, the water temperature grew, it flowed to the cooling part using a water transmission pipe and cooled again by the heat sink and a fan with a power of 3.1 W. The dimensions of the copper heat sink connected to the

a)

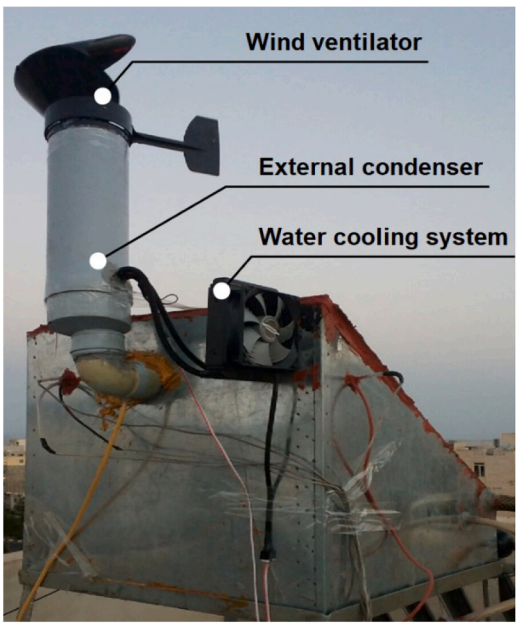

b)

Fig. 2. The solar desalination using ETHP-SC and external condenser a) front view b) back view.

Fig. 3. The configuration of manifold in the ETHP-SC.

copper sheet were 0.05 × 0.056 m^2. Fig. 3 indicates the manifold coupled with ETHP-SC of the modified solar still.

All measurements were performed in solar desalination under meteorology of Semnan (35° 33′ N, 53° 23′) for five days in July 2019. The hourly measurements were performed during experiments from 8:00 to 17:00. The depth of the water was 0.02 m at the beginning of each test, and the bottom of the tank was cleaned before each test. During the tests, solar intensity, ambient temperature, glass and water temperatures, external condenser temperature (perforated copper sheet connected to water cooling), wind velocity, freshwater yield of solar desalination and external condenser, total dissolved solids (TDS), and PH were measured.

Mathematical background

Thermal efficiency

The thermal efficiency of a solar desalination is the ratio of the water generation to the total energy entered the solar desalination through solar intensity and electrical consumption and is obtained by [40]:

$$\eta_{daily} = \frac{\dot{m}_{ev} h_{fg}}{I_t A_b + \dot{W}_{elec}} \tag{1}$$

where I_t is the cumulative daily solar intensity, $\dot{W}_{elec}$ is the electrical consumption of the instrument, h_{fg} is the latent heat, and A_b is the area of solar desalination and ETHP-SC.

Exergy analysis

The exergy analysis is the relation of the generated exergy to the sum of exergy input into the system and is calculated by [41]:

$$\eta_{Ex} = \frac{Ex_{Product}}{Ex_{input}} \tag{2}$$

The exergy input to the solar desalination is equal to:

$$Ex_{input} = I_t A_b \times \left[1 - \frac{4T_a}{3T_s} + \frac{1}{3}\left(\frac{T_a}{T_s}\right)^4\right] + \dot{W}_{elec} \tag{3}$$

where T_s denotes the sun's temperature, being equal to 5727 °C.

The exergy generation of the solar desalination is:

$$Ex_{product} = \frac{\dot{m}_{ev}}{3600} \times h_{fg} \times \left(1 - \frac{T_a}{T_w}\right) \quad (4)$$

Water production price

The water production price is a significant evaluating on the performance of a solar desalination. The capital recovery factor is obtained by [42]:

$$CRF = \frac{i(1+i)^n}{(1+i)^n - 1} \quad (5)$$

where i indicates the interest rate and is assumed 20%, and n shows the lifetime of the solar desalination (twenty years). The first annual price of the system is obtained by [43]:

$$FAC = P \times CRF \quad (6)$$

which P shows the capital price. The salvage value is obtained by the following formula [44]:

$$ASV = S \times SFF \quad (7)$$

where S denotes the salvage amount, being equal to twenty percent of the capital cost [45]. The sinking fund factor is given by [46]:

$$SFF = \frac{i}{(1+i)^n - 1} \quad (8)$$

The annual maintenance price, which includes the annual prices of the demolition of components and repairs of the solar desalination, which is equal to ten percentage of the first price, is calculated by [45]:

$$AMC = 0.10 \times FAC \quad (9)$$

The uniform annual price of solar desalination is obtained by [21]:

$$UAC = FAC + AMC - ASV \quad (10)$$

The price of one liter of water generation is obtained by [45]:

$$CPL = \frac{UAC}{M} \quad (11)$$

where M shows the annual freshwater generation of the system.

Benefit-cost ratio

This technique is an economic analysis of special finance projects and an applied technique to evaluate projects. The benefit-cost ratio is calculated by [47]:

$$BCR = \frac{UAB}{UAC} \quad (12)$$

where UAC and UAB show the present values of price and benefit, respectively. The present value of the benefit in solar desalination is obtained by [48]:

$$UAB = M \times POW \quad (13)$$

where M and POW respectively denote the annual freshwater yield of solar desalination and the purchase value of one liter of drinking freshwater, which varies in each country and equals 0.3$ in Iran.

Uncertainty analysis

All the experimental data were assumed to be divided uniformly. The standard uncertainty is obtained by [49,50]:

$$u = \frac{a}{\sqrt{3}} \quad (14)$$

Table 1
The standard uncertainty of the equipment.

Equipment	Accuracy	Range	Standard uncertainty
Solarimeter (W/m^2)	1	0–5000	0.6
Thermometer (°C)	0.1	−100 to 1300	0.06
PH meter	0.01	0–14	0.006
Conductivity meter (PPM)	1	0–2000	0.6
Volume meter (ml)	0.2	0–10	0.115
Multi meter (A)	0.01	0–15	0.006

where a resembles the accuracy of the equipment and u denotes the standard uncertainty. Table 1 lists the uncertainties related to the experimental convenience.

Klein [51] specified a relationship to obtain the uncertainty of the experimental data:

$$u(y) = \left[\left(\frac{\partial y}{x_1}\right)^2 .u^2(x_1) + \left(\frac{\partial y}{x_2}\right)^2 .u^2(x_2) + \cdots\right]^{0.5} \quad (15)$$

in which y indicates the function value of the input number x_i, and $u(x_i)$ shows the measured input values of x_i. By replacing the daily thermal efficiency into the equation (15), the uncertainty of thermal efficiency is obtained by:

$$u(\eta_{Energy}) = \left[\left(\frac{h_{fg}}{A_b I_t + \dot{W}_{elec}}\right)^2 .u^2\left(\dot{m}_{ev}\right) + \left(\frac{1}{(A_b I_t + \dot{W}_{elec})^2}\right)^2 .u^2(I_t) + \left(\frac{1}{(A_b I_t + \dot{W}_{elec})^2}\right)^2 .u^2\left(\dot{W}_{elec}\right)\right]^{0.5} \quad (16)$$

in which

$$u\left(\dot{W}_{pumps}\right) = \left[\frac{\dot{W}_{elec}^{\ 2}}{V^2}.u^2(V) + \frac{\dot{W}_{elec}^{\ 2}}{I^2}.u^2(I)\right]^{0.5} \quad (17)$$

where V shows the voltage and I shows the electrical current of the electrical equipment. Moreover, by replacing the exergy efficiency into the Klein equation, the uncertainty of exergy efficiency is obtained by:

$$u(\eta_{Exergy}) = \left[\left(\frac{1}{EX_{in}}\right)^2 .u^2(EX_{pr}) + \left(\frac{EX_{pr}}{EX_{in}^{\ 2}}\right)^2 .u^2(EX_{in})\right]^{0.5} \quad (18)$$

in which

$$u(EX_{pr}) = \left[\left(\dot{m}_{ev}\right)^2 .u^2(EX_{ev}) + (EX_{ev})^2 .u^2\left(\dot{m}_{ev}\right)\right]^{0.5} \quad (19)$$

$$u(EX_{ev}) = \left[\left(\frac{h_{fg}}{T_w}\right)^2 .u^2(T_a) + \left(\frac{h_{fg} T_a}{T_w^{\ 2}}\right)^2 .u^2(T_w)\right]^{0.5} \quad (20)$$

$$u(EX_{in}) = \left[\left(A_b\left(1 - \frac{4T_a}{3T_s} + \frac{1}{3}\left(\frac{T_a}{T_s}\right)^4\right)\right)^2 .u^2(I_t) + \left(A_b I_t\left(1 - \frac{4}{3T_s} + \frac{4}{3}\frac{T_a^3}{T_s^4}\right)\right)^2 .u^2(T_a) + u^2\left(\dot{W}_{elec}\right)\right]^{0.5} \quad (21)$$

By calculating the equations above, the highest uncertainties related to energy and exergy efficiencies in the solar desalination with external condenser and ETHP-SC equal 1.42% and 2.1%, respectively.

Energy payback time and energy product factor

The EPBT is the value of time which the energy or exergy produced of

a solar desalination generates to achieve the energy consumed to generate solar desalination products and components, which is calculated by the following equations [52]:

$$EPBT_{En} = \frac{E_{in}}{(E_{en})_{out}} \quad (22)$$

$$EPBT_{Ex} = \frac{E_{in}}{(E_{ex})_{out}} \quad (23)$$

where E_{in} indicates the embodied energy, and $(E_{ex})_{out}$ and $(E_{en})_{out}$ show the annual exergy and energy generation of the system, respectively. Furthermore, the EPF is the ratio of the total energy and exergy generated in the solar desalination to the embodied energy, which is calculated by [52]:

$$EPF_{En} = \frac{(E_{en})_{out}}{E_{in}} \quad (24)$$

$$EPF_{Ex} = \frac{(E_{ex})_{out}}{E_{in}} \quad (25)$$

Exergoeconomic parameter

The exergoeconomic analysis can be specified as the coupled of economic analysis using exergy analysis in the system, which is obtained by [53]:

$$R_{Ex} = \frac{(E_{ex})_{out}}{UAC} \quad (26)$$

$$R_{En} = \frac{(E_{en})_{out}}{UAC} \quad (27)$$

where R_{Ex}, and R_{En} show the exergoeconomic parameter considering exergy and energy, respectively.

CO_2 emission

The CO_2 emission per kWh is about 0.96 kg [54]. The CO_2 generation per kWh is approximately 2 kg, considering the transfer loss and distribution loss, which are caused by unsuitable device. The annual CO_2 emission and CO_2 emission over the lifetime of the system are given as [55]:

$$ACDE = \frac{2 \times E_{in}}{n} \quad (28)$$

$$CDED = 2 \times E_{in} \quad (29)$$

CO_2 removal

The CO_2 removal rate in the solar desalination is equal to $(E_{en})_{out} \times 2$. Thus, the CO_2 removal during the lifetime of a solar desalination is $(E_{en})_{out} \times 2 \times n$. The net value of CO_2 removal during the lifetime of a solar desalination is calculated by [56]:

$$X_{co_2} = \frac{2((E_{en})_{out} \times n - E_{in})}{1000} \quad (30)$$

where X_{co_2} shows the environmental parameter.

Enviroeconomic parameter

The enviroeconomic analysis is obtained by multiplying the international price of CO_2 by CO_2 removal during the lifetime of a solar desalination, which is calculated by [57]:

$$Z_{co_2} = z_{co_2} \times X_{co_2} \quad (31)$$

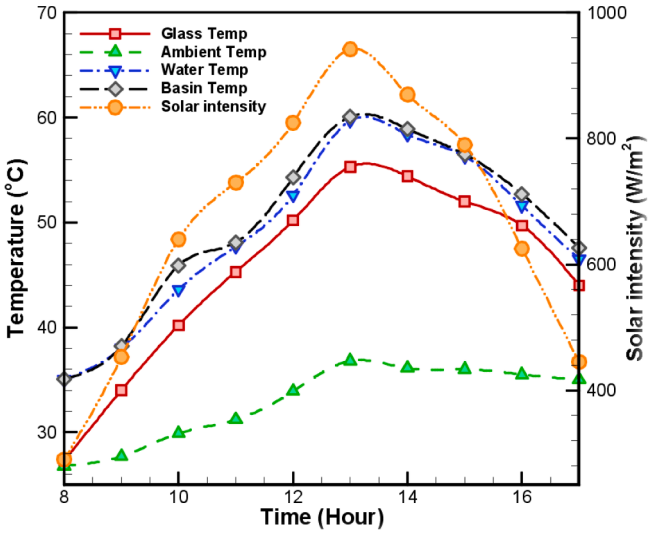

Fig 4. Variation of temperature and solar intensity of traditional solar still.

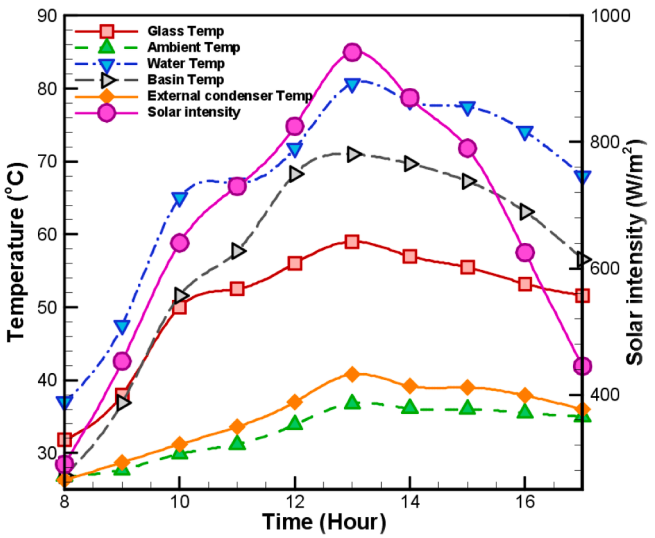

Fig. 5. Variation of temperature and solar intensity in solar still coupled with external condenser and ETHP-SC.

where Z_{co_2} shows the enviroeconomic parameter, and z_{co_2} shows the international cost of carbon, which is about $14.5 per ton [58].

Exergoenvironmental analysis

The exergoenvironmental parameter gives the CO_2 mitigation considering exergy in a solar desalination. The exergoenvironmental parameter is calculated by [58]:

$$X_{ex,co_2} = \frac{2((E_{ex})_{out} \times n - E_{in})}{1000} \quad (32)$$

where X_{ex,co_2} is the exergoenvironmental parameter based on exergy.

Exergoenviroeconomic analysis

The exergoenviroeconomic analysis is a technique to assess the cost resulting of CO_2 emissions considering the exergy, which is obtained by [59]:

$$Z_{ex,co_2} = z_{co_2} \times X_{x,co_2} \quad (33)$$

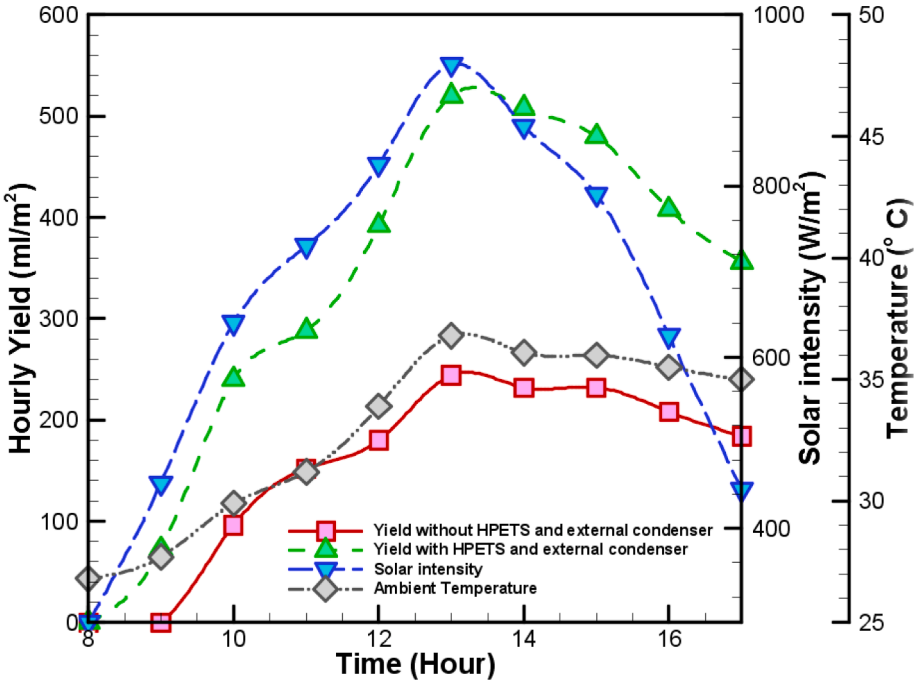

Fig. 6. Hourly yield of solar stills with respect to solar radiation and ambient temperature.

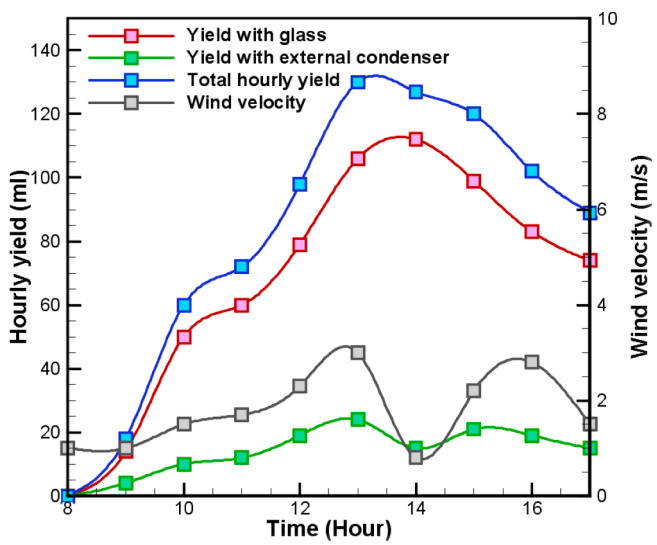

Fig. 7. Hourly water productivity with glass cover and external condenser respect to wind velocity.

where Z_{ex,co_2} is the exergoenviroeconomic parameter.

Results and discussion

Solar radiation, environment temperature, and wind velocity are the parameters that impact the productivity of solar desalination. An increase in sun intensity raises the temperature of different components of a solar desalination. Figs. 4 and 5 indicate the variation of solar intensity and temperature of various components of both solar stills. Based on the results, the saline water temperature was higher than absorber plate temperature in the solar desalination with external condenser and ETHP-SC, while being lower than absorber plate temperature in the conventional ones, due to recirculation of water between the manifold of ETHP-SC and solar still. Moreover, the external condenser temperature was approximately 15.5 °C less than the glass temperature of the solar still with ETHP-SC and external condenser. Moreover, the largest temperature difference between brackish water and external condenser was about 39.9 °C, while being about 22 °C between the water and glass. The highest water temperature was about 80.7 °C and 59.7 °C in the solar desalination with external condenser and ETHP-SC and conventional solar desalination, respectively, which were achieved at the solar radiation of 942 W/m^2.

Fig. 6 indicates the hourly productivity of traditional and modified solar desalination with respect to solar radiation and ambient temperature. The behavior of hourly yield of modified and conventional solar desalination is the same at different hours. The maximum freshwater yield of solar desalination with external condenser and ETHP-SC and conventional solar desalination was about 520 ml/m^2 and 244 ml/m^2, which achieved at the solar radiation of 942 W/m^2, respectively. The daily yield of the solar desalination with external condenser and ETHP-SC was always more than that of the traditional solar desalination, due to the use of external condenser and ETHP-SC in the modified solar still. Moreover, solar radiation had a direct effect on water productivity in both solar desalinations.

Fig. 7 indicates the hourly yield of two condensation areas (external condenser and glass) in the solar desalination using external condenser and evacuated tube heat pipe solar collector. The water generation in the glass is related to the temperature difference of the water and glass, while the water generation in the external condenser is related to the wind velocity and the temperature difference between the external condenser (perforated copper sheet connected to water cooling system) and water. The input flow of water vapor to the external condenser increased with the wind speed in the solar still. The hourly water productivity of the external condenser was directly affected by the wind speed. The highest water productivity of the external condenser was about 24 ml, which occurred at a wind velocity of about 2.9 m/s, while the lowest water productivity was about 15 ml, which occurred at a wind velocity of 0.8 m/s. The yield fraction of the external condenser was approximately 17.6% of the total productivity in the modified solar desalination.

Fig. 8 indicates the variations in water productivity of the external condenser, wind velocity, and suction flow rate of the wind ventilator of

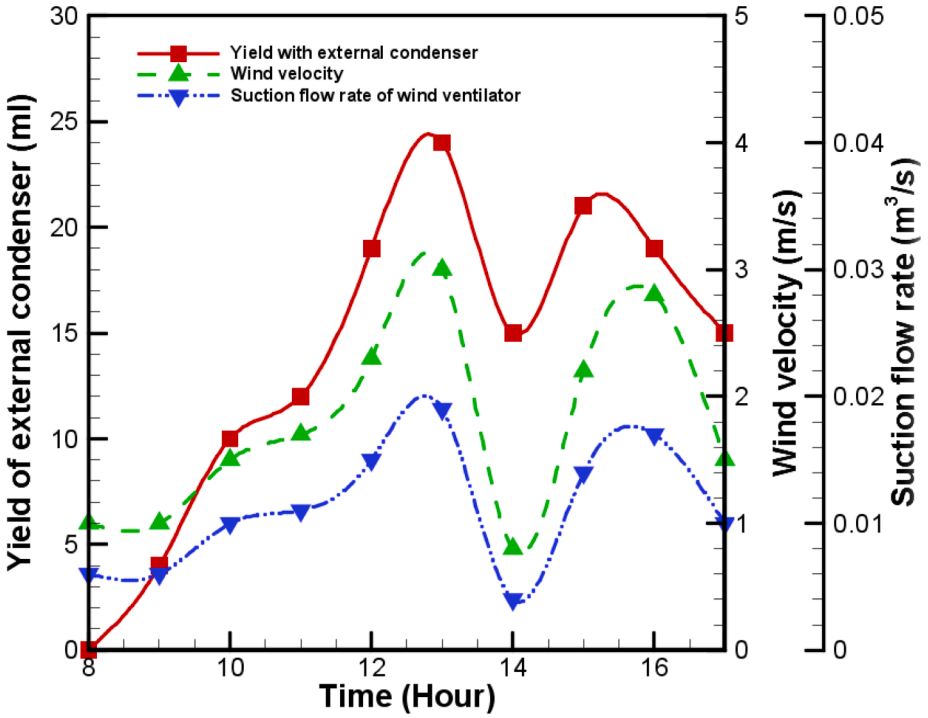

Fig. 8. Hourly variation of water productivity of external condenser, wind velocity and suction flow rate of wind ventilator.

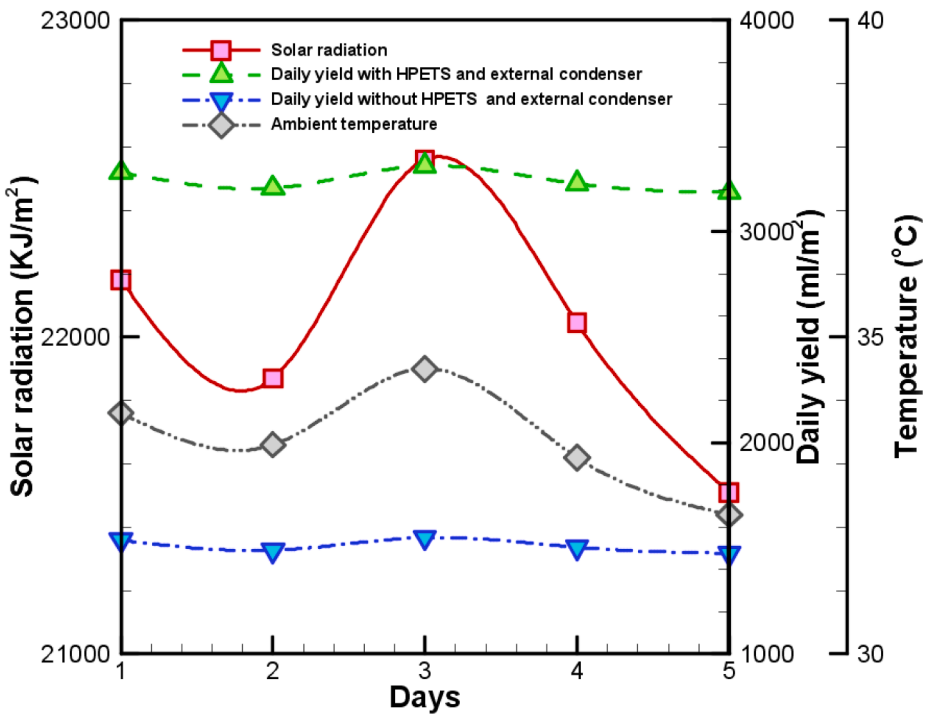

Fig. 9. Daily yield, solar intensity and ambient temperature of solar stills.

the modified solar desalination. As observed, the behavior of water yield of external condenser, wind velocity, and the suction flow rate was the same at various hours. Moreover, the maximum productivity of the external condenser was about 24 ml, which occurred at a wind velocity of 2.9 m/s and a suction flow rate of 0.019 m^3/s in the wind ventilator.

Fig. 9 indicates the variations of freshwater yield, solar intensity, and average ambient temperature within five days in July. The results indicated that the freshwater yield was straightly affected by the cumulative solar intensity and average ambient temperature. Moreover, due to the use of ETHP-SC and external condenser to increase water temperature and condensation rate, respectively, in the modified solar desalination, its water generation was about 213% more than that in the solar desalination without any modifications.

Fig. 10 illustrates the variations of total daily yield of solar desalination with ETHP-SC and external condenser, wind speed, and water productivity fraction of external condenser of modified solar

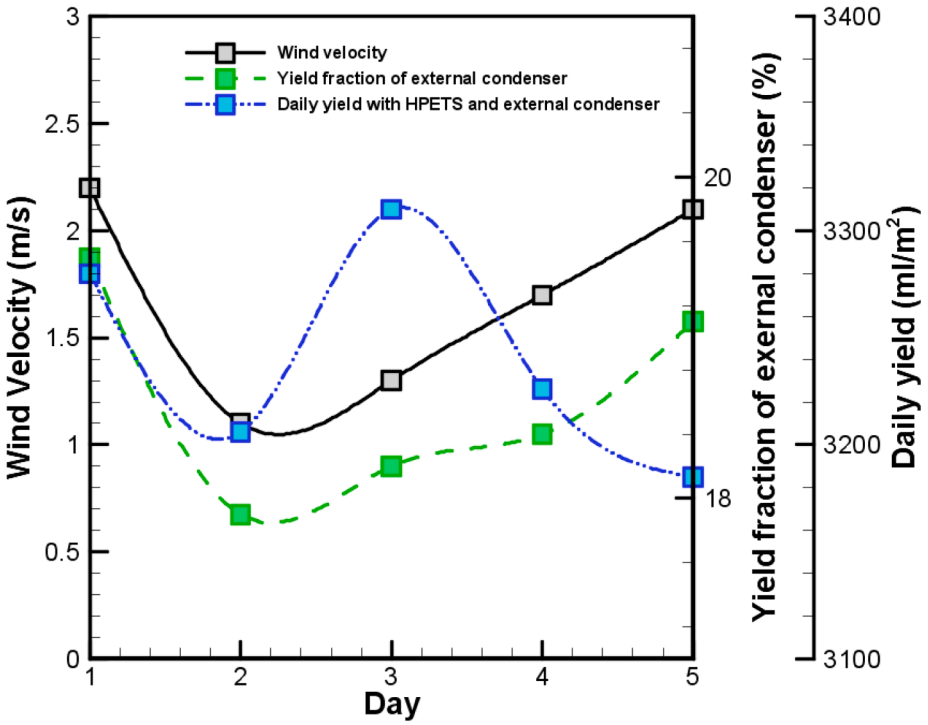

Fig. 10. Variation of wind velocity and yield fraction of external condenser in different days.

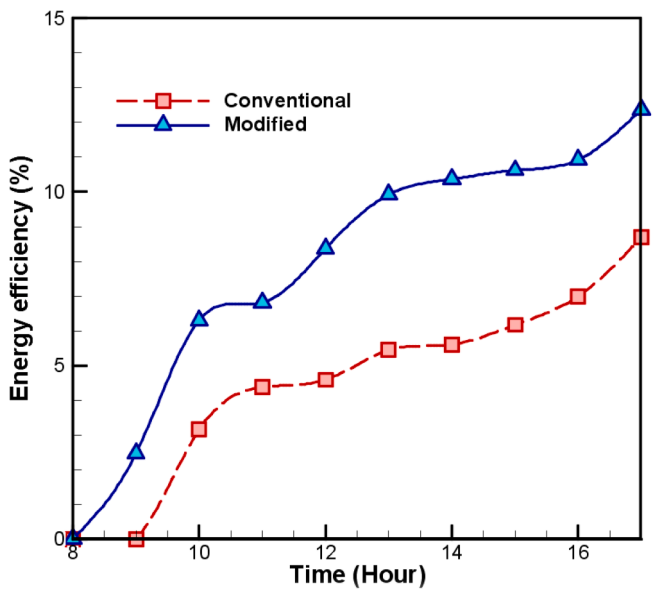

Fig. 11. The thermal energy efficiency of solar desalinations.

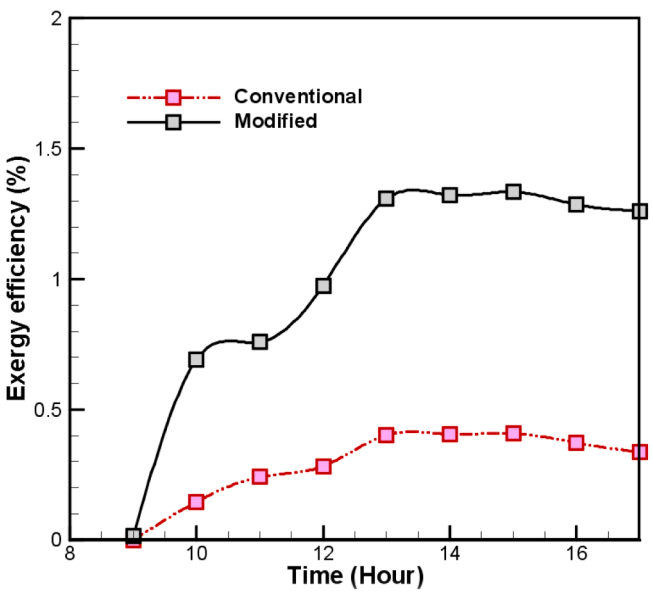

Fig. 12. The exergy efficiency of solar desalinations.

desalination during the five days of experiments. As observed, the productivity fraction of the external condenser had a positive impact on the wind speed. The maximum and minimum water productivity fractions of the external condenser were about 19.5% and 17.9 %, which occurred at average wind speeds of 2.2 m/s and 1.1 m/s, respectively. Moreover, the average yield fraction of the external condenser was approximately 18.62% of total production in the solar still with external condenser and ETHP-SC.

Fig. 11 indicates the hourly change of the thermal efficiency for solar desalination with ETHP-SC and external condenser and conventional solar stills. The results indicated that the energy efficiency of solar desalination with ETHP-SC and external condenser was higher than the traditional still. This was due to the more amount of water generated by the solar desalination with ETHP-SC and external condenser. Moreover, in the last hours of the experiments, the solar radiation was reduced by the rise in energy efficiency. This was caused by the high water temperature of the solar desalination with ETHP-SC and external condenser.

Fig. 12 demonstrates the changes in the exergy efficiency in both solar desalinations. As observed, the behavior of the exergy efficiency was the same in both systems during the tests. The exergy efficiency of the solar desalination with external condenser and ETHP-SC was more than the traditional solar desalination due to the more freshwater generation. Furthermore, the exergy efficiency of solar desalination with ETHP-SC and external condenser and conventional solar desalination

Table 2
Parameters of coefficient of the proposed model of solar stills.

Type of solar still	n_1	A	b	c	R^2	Maximum Error (%)
Modified	1.06 E-04	1.05	−0.075	0.016	0.992	0.53
Conventional	2.19 E-8	1.95	−0.432	0.032	0.997	1.05

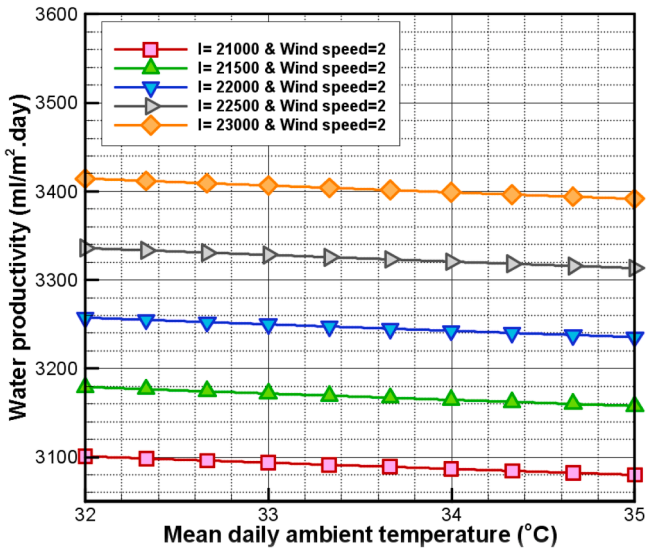

a)

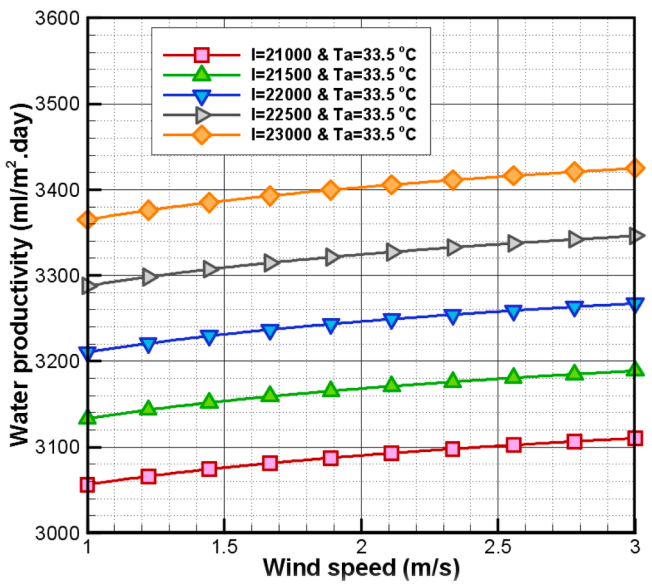

b)

Fig. 13. The impact of a) average ambient temperature and b) wind speed on the water productivity of proposed model.

equaled 1.3% and 0.4%, respectively, at 13:00.

According to the results shown in Figs. 9 and 10 using the regression method, the daily yield of solar desalinations can be estimated as a function of cumulative solar intensity, average ambient temperature, and wind velocity:

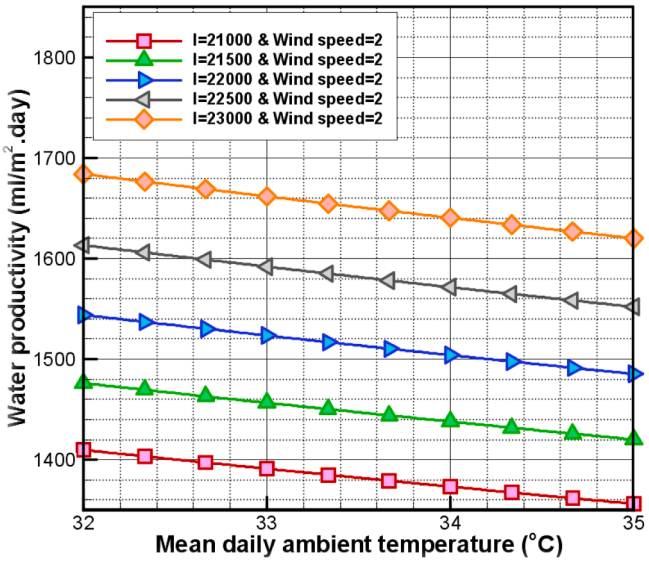

a)

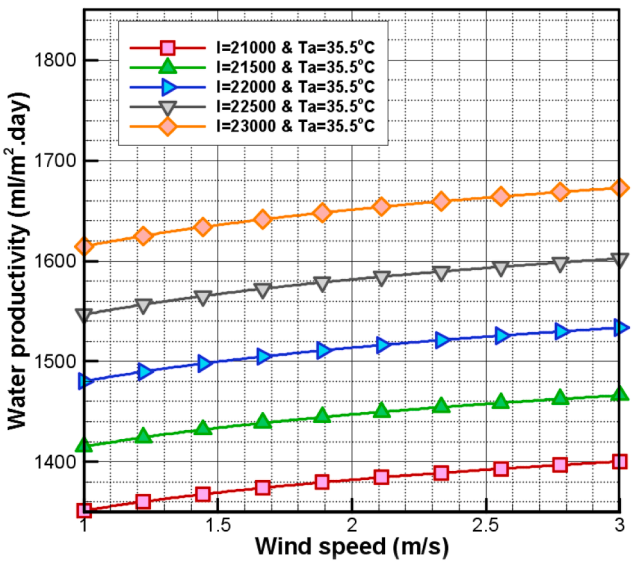

b)

Fig. 14. The impact of a) mean daily ambient temperature and b) wind speed on the water productivity of proposed model.

$$\dot{m}_{daily} = n_1 \times I^a \times T_a{}^b \times V_{wind}^c \quad (34)$$

where $\dot{m}_{daily}$ is the freshwater production of the solar desalination, I is the cumulative solar intensity, and T_a is the average ambient temperature. Table 2 shows the parameters a, b, c, and errors related to the equation. This equation is used to estimate the water yield of solar still in various weather conditions.

Figs. 13 and 14 demonstrate the impact of average ambient temperature and wind velocity on freshwater productivity in various cumulative solar intensities of conventional and modified solar desalination, respectively. As observed, that the water output of the solar desalination had an opposite impact on the mean ambient temperature due to the raise in the glass temperature, which reduced the temperature difference between the glass and brackish water. Furthermore, the rise in the wind speed enhanced the freshwater generation by

Table 3
Construction Cost of solar desalinations.

Type of solar desalination	Cost of components ($)	Salvage Value ($)
Modified		
Glass	9	1.8
Pumps	24	4.8
Body	45	9
Wind powered ventilator	10	2
manifold	15	3
PVC pipe	4	0.8
Water cooling system	40	8
External Condenser (Copper)	10	2
evacuated tube heat pipe solar collector	70	14
Photovoltaic panel	40	8
insulation	5	1
Galvanized (Support)	20	4
Total Cost	292	58.4
Conventional		
Glass	9	1.8
insulation	5	1
Body	45	9
Galvanized (Support)	20	4
Total cost	79	15.8

increasing the flow rate of water vapor to the external condenser, which raised the value of water produced in the external condenser.

Table 3 shows the construction cost of solar stills. As can be seen, the construction cost in the solar desalination with ETHP-SC and external condenser, and the conventional solar desalination equaled $292 and $79, respectively. Table 4 illustrates the cost per liter of solar stills with interest rates of 10% and 20% during lifetimes of 10 and 20 years. As observed, the highest cost per liter in solar desalination with ETHP-SC and external condenser and traditional solar still was about 0.0653 $/l/m^2 and 0.0378 $/l/m^2, respectively. Also, the CPL of the solar desalination with ETHP-SC and external condenser was higher compared to the conventional ones and occurred at an interest rate of 20% and a lifetime of ten years.

Table 5 indicates the benefit-cost ratio of solar stills with interest rates of 10% and 20% and lifetimes of 10 and 20 years. The benefit-cost ratios in the solar desalination with ETHP-SC and external condenser and conventional solar desalination were higher than one. Furthermore, the interest rate and lifetime had inverse effects on the benefit-cost ratio in the solar desalination with ETHP-SC and external condenser and conventional solar desalination.

Table 6 presents the embodied energy of solar desalination. The energy used to generate various parts in the solar desalination with ETHP-SC and external condenser and conventional solar desalination was about 630.3 kWh and 132.3 kWh, respectively. As observed, the embodied energy in the modified solar desalination was 4.76 times higher than that in the conventional ones.

Table 7 indicates the EPBT and EPF based on exergy and energy outputs. According to the results, the EPBT considering energy and exergy was 0.82 and 14.20 years in the modified solar still and 0.37 and 6.37 years in the conventional solar desalination, respectively. This is due to the high embodied energy of the modified solar desalination compared to the conventional ones. The results also showed that the EPF based on energy and exergy equaled 1.20 and 0.07 in the solar desalination with ETHP-SC and external condenser and 2.69 and 0.15 in the conventional solar still, respectively.

Table 8 indicates the exergoeconomic data for various lifetimes and interest rates of solar desalinations. As observed, the exergoeconomic parameter in the modified solar still was lower than the modified solar still in different cases, which was due to the more construction cost in the modified solar desalination. Furthermore, the exergoeconomic parameters based on energy at an interest rate of 20% and a lifetime of 20 years in the solar desalination with ETHP-SC and external condenser and the conventional one were equal to 11.09 kWh/$ and 19.19 kWh/$, respectively.

Table 9 presents the environmental parameters for the lifetime of 20 years in the solar stills. It can be seen that the CO_2 removal of the system with ETHP-SC and external condenser was about 2.13 times that of the traditional one. Moreover, the CO_2 removal based on exergoenvironmental analysis in the solar desalination with ETHP-SC and external condenser and traditional solar desalination equaled 0.51 and 0.57 tons, respectively. Moreover, the total dissolved solids and pH were measured in two days, whose results are illustrated in Table 10. According to the results, the output freshwater had good quality in the traditional solar

Table 4
Water production cost of solar desalinations.

Type of solar desalination	n (year)	i (%)	CRF	FAC	SSF	S	ASV	AMC	UAC	M (l/m^2.year)	CPL ($/l/m^2)
Modified											
	10	0.10	0.163	47.522	0.063	58.400	3.664	7.128	50.986	1191	0.0428
	10	0.20	0.239	69.649	0.039	58.400	2.250	10.447	77.846	1191	0.0653
	20	0.10	0.117	34.298	0.017	58.400	1.020	5.145	38.423	1191	0.0323
	20	0.20	0.205	59.964	0.005	58.400	0.313	8.995	68.646	1191	0.0576
Conventional											
	10	0.10	0.163	12.857	0.063	15.800	0.991	1.929	13.794	557	0.0247
	10	0.20	0.239	18.843	0.039	15.800	0.609	2.826	21.061	557	0.0378
	20	0.10	0.117	9.279	0.017	15.800	0.276	1.392	10.395	557	0.0186
	20	0.20	0.205	16.223	0.005	15.800	0.085	2.433	18.572	557	0.0333

Table 5
Benefit cost ratio of solar stills.

Type of solar still	n (year)	i (%)	UAC ($)	POW ($)	Annual water productivity (L)	UAB ($)	B/C
Modified							
	10	0.10	50.986	0.3	297	89.1	1.75
	10	0.20	77.846	0.3	297	89.1	1.14
	20	0.10	38.423	0.3	297	89.1	2.32
	20	0.20	68.646	0.3	297	89.1	1.30
Conventional						0	
	10	0.10	13.794	0.3	140	42	3.04
	10	0.20	21.061	0.3	140	42	1.99
	20	0.10	10.395	0.3	140	42	4.04
	20	0.20	18.572	0.3	140	42	2.26

Table 6
Embodied energy of different part of solar desalination [52,60,61].

Type of solar still	Name of Component	Energy density		Mass of component (kg)	Embodiedenergy (kWh)
		MJ/kg	kWh/kg		
Modified					
	Glass	101.8	28.3	2	56.6
	pumps (PVC)	77.2	21.4	0.4	8.5
	Manifold (Steel)	25	6.9	2	13.8
	Wind powered ventilator (PVC)	77.2	21.4	1	21.4
	External Condenser (Copper)	100	27.7	0.3	8.3
	Body (Steel)	25	6.9	6	41.4
	Water cooling system (copper)	100	27.7	0.1	2.7
	Water cooling system (steel)	25	6.9	1.6	11.1
	evacuated tube heat pipe	11128.7 kWh/m^3		0.03 m^3	334
	Insulation	55.6	15.44	0.3	4.63
	Photovoltaic panel	980 kWh/m^2		0.1 m^2	98
	pipe (PVC)	77.2	21.4	0.1	2.1
	Support (Galvanized)	50	13.9	2	27.8
	Total Embodied energy (kWh)	–	–	–	630.3
Conventional					
	Glass	31.5	28.3	2	56.6
	Body	25	6.9	6	41.4
	Insulation	55.6	15.44	0.3	4.63
	PVC pipe	77.2	21.4	0.1	2.1
	Support (Galvanized)	50	13.9	2	27.8
	Total Embodied energy (kWh)	–	–	–	132.3

Table 7
EPBT and EPF of solar stills.

Type of solar still	Annual yield (l/m^2.year)	Embodied Energy (kWh)	Annual$(E_{en})_{out}$ (kWh)	Annual$(E_{ex})_{out}$ (kWh)	$EPBT_{En}$	$EPBT_{Ex}$	EPF_{En}	EPF_{Ex}
Modified	1191	630.3	761.1	44.36	0.82	14.20	1.20	0.07
Conventional	557	132.3	356.3	20.77	0.37	6.37	2.69	0.15

Table 8
Exergoeconomic parameter for solar stills.

Type of solar still	n (year)	i (%)	Annual$(E_{en})_{out}$ (kWh)	Annual$(E_{ex})_{out}$ (kWh)	UAC	$R_{En}\left(\frac{kWh}{\$}\right)$	$R_{Ex}\left(\frac{kWh}{\$}\right)$
Modified							
	10	0.10	761.1	44.36	50.986	14.93	0.87
	10	0.20	761.1	44.36	77.846	9.78	0.57
	20	0.10	761.1	44.36	38.423	19.81	1.15
	20	0.20	761.1	44.36	68.646	11.09	0.65
Conventional							
	10	0.10	356.3	20.77	13.794	25.83	1.51
	10	0.20	356.3	20.77	21.061	16.92	0.99
	20	0.10	356.3	20.77	10.395	34.28	2.00
	20	0.20	356.3	20.77	18.572	19.19	1.12

desalination and solar desalination with ETHP-SC and external condenser.

Comparison of the distilled water productivity and total cost of water production in the present study and different types of solar stills presented in Table 11. According to Table 11, although the cost of water production for modified solar desalination is higher than conventional type, its annual distilled water productivity is also higher.

Conclusion

In this research, the modified and conventional solar desalinations have been experimentally investigated. The ETHP-SC was used to raise the saline water temperature, while a new design of external condenser was employed to improve the condensation rate. The water vapor was discharged from the enclosure of the solar still by the wind ventilator and then distilled by hitting the perforated copper sheet that was connected to cooling water. All measurements were performed on solar still with ETHP-SC and external condenser, and conventional solar stills in Semnan climatic conditions (35° 33′ N, 53° 23′) in July 2019 during five days. The water productivity, and economic and environmental analysis of the solar desalination using ETHP-SC and external condenser were also compared with those of the traditional ones. The significant results of the experiments in this study are as follows:

- The freshwater generation of the solar desalination using ETHP-SC and external condenser was increased by 213% in comparison to the traditional system.
- The CPL of the solar still with modification and the conventional one were equal to 0.0576 \$/l/m^2 and 0.0333 \$/l/m^2, respectively.
- The energy and exergy efficiencies of the solar desalination with ETHP-SC and external condenser was more than the conventional solar desalination.
- The freshwater generation of solar desalination was directly affected by wind speed.
- The average yield fraction of using a wind ventilator and water cooling system (external condenser) was about 18.62% of the total yield in the solar still with modification.

Table 9
Environmental Analysis of solar desalinations.

Parameter	Solar desalination with ETHP-SC and external condenser	Conventional solar desalination
Life span (years)	20	20
Embodied Energy (kWh)	630.3	132.3
Annual Energy generation (kWh)	761.1	356.3
Annual Exergy generation (kWh)	44.36	20.77
CO_2 emission during lifetime (kg)	1260.6	264.6
CO_2 removal during lifetime (tons)	30.45	14.25
Environmental parameter (ton Co_2)	29.19	13.99
Enviroeconomic parameter ($)	423.19	202.83
Exergoenvironmental parameter (ton Co_2)	0.51	0.57
Exergoenviroeconomic parameter ($)	7.45	8.21

Table 10
The quality of water

	Day 1		Day 4	
	Total dissolved solid (ppm)	PH	Total dissolved solid (ppm)	PH
Saline water	855	7.8	789	8.01
Produced water	121	7.18	131	7.21

Table 11
Comparison distilled water productivity and total cost of solar still

Reference	Distilled water productivity (l/m^2. year)	CPL ($/L. m^2)
[17]	547	0.19
[19]	710	0.03
[18]	438	0.13
[26]	944	–
[26]	1600	–
[53]	180	0.18
Present study-Conventional	557	0.03
Present study-Modified	1191	0.06

- The benefit cost ratios in both solar desalination were higher than unity.
- The CO_2 removal based on environmental parameter in the modified and conventional solar desalination was about 29.19 tons and 13.99 tons, respectively.

CRediT authorship contribution statement

Shahin Shoeibi: Methodology, Software, Conceptualization, Formal analysis, Writing – review & editing. **Hadi Kargarsharifabad:** Software, Conceptualization, Formal analysis, Visualization, Supervision, Validation, Project administration, Writing – review & editing. **Nader Rahbar:** Resources, Validation, Writing – review & editing. **Gholamreza Khosravi:** Resources, Validation, Writing – review & editing. **Mohsen Sharifpur:** Resources, Validation, Writing – review & editing.

Declaration of Competing Interest

The authors declare that they have no known competing financial interests or personal relationships that could have appeared to influence the work reported in this paper.

References

[1] Sarafraz M, Tlili I, Abdul Baseer M, Safaei MR. Potential of solar collectors for clean thermal energy production in smart cities using nanofluids: experimental assessment and efficiency improvement. Appl Sci 2019;9:1877.
[2] Khanmohammadi S, Khanjani S. Experimental study to improve the performance of solar still desalination by hydrophobic condensation surface using cold plasma technology. Sustainable Energy Technol Assess 2021;45:101129.
[3] Hassan H, Yousef MS, Fathy M. Productivity, exergy, exergoeconomic, and enviroeconomic assessment of hybrid solar distiller using direct salty water heating. Environ Sci Pollut Res Int 2021;28:5482–94.
[4] Pourkiaei SM, Ahmadi MH, Ghazvini M, Moosavi S, Pourfayaz F, Kumar R, et al. Status of direct and indirect solar desalination methods: comprehensive review. Eur Phys J Plus 2021;136:1–36.
[5] Fath HES, El-Samanoudy M, Fahmy K, Hassabou A. Thermal-economic analysis and comparison between pyramid-shaped and single-slope solar still configurations. Desalination 2003;159:69–79.
[6] Shoeibi S, Rahbar N, Abedini Esfahlani A, Kargarsharifabad H. Improving the thermoelectric solar still performance by using nanofluids– Experimental study, thermodynamic modeling and energy matrices analysis. Sustain Energy Technol Assess 2021;47:101339.
[7] Shoeibi S, Kargarsharifabad H, Rahbar N. Effects of nano-enhanced phase change material and nano-coated on the performance of solar stills. J Storage Mater 2021; 42:103061.
[8] Thakur AK, Sathyamurthy R, Sharshir SW, Kabeel AE, Elkadeem MR, Ma Z, et al. Performance analysis of a modified solar still using reduced graphene oxide coated absorber plate with activated carbon pellet. Sustainable Energy Technol Assess 2021;45:101046.
[9] Tiwari AK, Tiwari GN. Effect of water depths on heat and mass transfer in a passive solar still: in summer climatic condition. Desalination 2006;195:78–94.
[10] Phadatare MK, Verma SK. Influence of water depth on internal heat and mass transfer in a plastic solar still. Desalination 2007;217:267–75.
[11] Goshayeshi HR, Safaei MR. Effect of absorber plate surface shape and glass cover inclination angle on the performance of a passive solar still. Int J Numer Meth Heat Fluid Flow 2019;30:3183–98.
[12] Jathar LD, Ganesan S, Shahapurkar K, Soudagar MEM, Mujtaba M, Anqi AE, et al. Effect of various factors and diverse approaches to enhance the performance of solar stills: a comprehensive review. J Therm Anal Calorim 2021;1–32.
[13] Khalifa AJN, Hamood AM. Effect of insulation thickness on the productivity of basin type solar stills: an experimental verification under local climate. Energy Convers Manage 2009;50:2457–61.
[14] Cuce PM, Cuce E, Tonyali A. Performance analysis of a novel solar desalination system – Part 2: The unit with sensible energy storage with thermal insulation and cooling system. Sustainable Energy Technol Assess 2021;48:101674.
[15] Mashaly AF, Alazba AA. Thermal performance analysis of an inclined passive solar still using agricultural drainage water and artificial neural network in arid climate. Sol Energy 2017;153:383–95.
[16] Abu-Arabi M, Al-harahsheh M, Ahmad M, Mousa H. Theoretical modeling of a glass-cooled solar still incorporating PCM and coupled to flat plate solar collector. J Storage Mater 2020;29:101372.
[17] Shalaby SM, El-Bialy E, El-Sebaii AA. An experimental investigation of a v-corrugated absorber single-basin solar still using PCM. Desalination 2016;398: 247–55.
[18] Safaei MR, Goshayeshi HR, Chaer I. Solar still efficiency enhancement by using graphene oxide/paraffin nano-PCM. Energies 2019;12:2002.
[19] Bait O. Direct and indirect solar–powered desalination processes loaded with nanoparticles: a review. Sustainable Energy Technol Assess 2020;37:100597. https://doi.org/10.1016/j.seta.2019.100597.
[20] Sarafraz MM, Tlili I, Tian Z, Bakouri M, Safaei MR, Goodarzi M. Thermal evaluation of graphene nanoplatelets nanofluid in a fast-responding HP with the potential use in solar systems in smart cities. Appl Sci 2019;9:2101.
[21] Shoeibi S, Rahbar N, Esfahlani AA, Kargarsharifabad H. Energy matrices, exergoeconomic and enviroeconomic analysis of air-cooled and water-cooled solar still: experimental investigation and numerical simulation. Renewable Energy 2021;171:227–44.
[22] Shoeibi S, Rahbar N, Abedini Esfahlani A, Kargarsharifabad H. A review of techniques for simultaneous enhancement of evaporation and condensation rates in solar stills. Sol Energy 2021;225:666–93.
[23] Rubio E, Porta MA, Fernández JL. Cavity geometry influence on mass flow rate for single and double slope solar stills. Appl Therm Eng 2000;20:1105–11.
[24] Abdullah AS. Improving the performance of stepped solar still. Desalination 2013; 319:60–5.
[25] Arora S, Singh HP, Sahota L, Arora MK, Arya R, Singh S, et al. Performance and cost analysis of photovoltaic thermal (PVT)-compound parabolic concentrator (CPC) collector integrated solar still using CNT-water based nanofluids. Desalination 2020;495:114595.

[26] Sarafraz M, Tlili I, Tian Z, Bakouri M, Safaei MR. Smart optimization of a thermosyphon heat pipe for an evacuated tube solar collector using response surface methodology (RSM). Phys A 2019;534:122146.
[27] Bhargva M, Yadav A. Effect of shading and evaporative cooling of glass cover on the performance of evacuated tube-augmented solar still. Environ Dev Sustain 2020;22:4125–43.
[28] Bhargva M, Yadav A. Productivity augmentation of single-slope solar still using evacuated tubes, heat exchanger, internal reflectors and external condenser. Energy Sources Part A 2019:1–21.
[29] Feilizadeh M, Estahbanati MRK, Khorram M, Rahimpour MR. Experimental investigation of an active thermosyphon solar still with enhanced condenser. Renewable Energy 2019;143:328–34.
[30] Khairat Dawood MM, Nabil T, Kabeel AE, Shehata AI, Abdalla AM, Elnaghi BE. Experimental study of productivity progress for a solar still integrated with parabolic trough collectors with a phase change material in the receiver evacuated tubes and in the still. J Storage Mater 2020;32:102007.
[31] Fallahzadeh R, Aref L, Gholamiarjenaki N, Nonejad Z, Saghi M. Experimental investigation of the effect of using water and ethanol as working fluid on the performance of pyramid-shaped solar still integrated with heat pipe solar collector. Sol Energy 2020;207:10–21.
[32] Singh DB, Tiwari GN. Energy, exergy and cost analyses of N identical evacuated tubular collectors integrated basin type solar stills: a comparative study. Sol Energy 2017;155:829–46.
[33] Eltawil MA, Omara ZM. Enhancing the solar still performance using solar photovoltaic, flat plate collector and hot air. Desalination 2014;349:1–9.
[34] Kabeel AE, Omara ZM, Essa FA. Enhancement of modified solar still integrated with external condenser using nanofluids: an experimental approach. Energy Convers Manage 2014;78:493–8.
[35] Kabeel AE, Omara ZM, Essa FA. Numerical investigation of modified solar still using nanofluids and external condenser. J Taiwan Inst Chem Eng 2017;75:77–86.
[36] Omara ZM, Kabeel AE, Essa FA. Effect of using nanofluids and providing vacuum on the yield of corrugated wick solar still. Energy Convers Manage 2015;103:965–72.
[37] Hassan H, Ahmed MS, Fathy M, Yousef MS. Impact of salty water medium and condenser on the performance of single acting solar still incorporated with parabolic trough collector. Desalination 2020;480:114324.
[38] Bhardwaj R, ten Kortenaar MV, Mudde RF. Maximized production of water by increasing area of condensation surface for solar distillation. Appl Energy 2015;154:480–90.
[39] Rastegar S, Kargarsharifabad H, Rahbar N, Shafii MB. Distilled water production with combination of solar still and thermosyphon heat pipe heat exchanger coupled with indirect water bath heater – experimental study and thermoeconomic analysis. Appl Therm Eng 2020;176:115437.
[40] Kabeel AE. Performance of solar still with a concave wick evaporation surface. Energy 2009;34:1504–9.
[41] Petela R. Exergy of undiluted thermal radiation. Sol Energy 2003;74:469–88.
[42] El-Said EMS, Elshamy SM, Kabeel AE. Performance enhancement of a tubular solar still by utilizing wire mesh packing under harmonic motion. Desalination 2020;474:114165.
[43] Rahbar N, Gharaiian A, Rashidi S. Exergy and economic analysis for a double slope solar still equipped by thermoelectric heating modules - an experimental investigation. Desalination 2017;420:106–13.
[44] Saini V, Sahota L, Jain VK, Tiwari GN. Performance and cost analysis of a modified built-in-passive condenser and semitransparent photovoltaic module integrated passive solar distillation system. J Storage Mater 2019;24:100809.
[45] Shoeibi S, Rahbar N, Abedini Esfahlani A, Kargarsharifabad H. Application of simultaneous thermoelectric cooling and heating to improve the performance of a solar still: an experimental study and exergy analysis. Appl Energy 2020;263:114581.
[46] Rahbar N, Esfahani JA. Experimental study of a novel portable solar still by utilizing the heatpipe and thermoelectric module. Desalination 2012;284:55–61.
[47] Kosmadakis G, Manolakos D, Kyritsis S, Papadakis G. Economic assessment of a two-stage solar organic Rankine cycle for reverse osmosis desalination. Renewable Energy 2009;34:1579–86.
[48] Singh AK, Poonia S, Jain D, Mishra D. Performance evaluation and economic analysis of solar desalination device made of building materials for hot arid climate of India. Desalin Water Treat 2019;141:36–41.
[49] Hasani M, Rahbar N. Application of thermoelectric cooler as a power generator in waste heat recovery from a PEM fuel cell – An experimental study. Int J Hydrogen Energy 2015;40:15040–51.
[50] Rahbar N, Asadi A. Solar intensity measurement using a thermoelectric module; experimental study and mathematical modeling. Energy Convers Manage 2016;129:344–53.
[51] P. Fornasini. The uncertainty in physical measurements: an introduction to data analysis in the physics laboratory. Springer Science & Business Media 2008.
[52] Yousef MS, Hassan H. Assessment of different passive solar stills via exergoeconomic, exergoenvironmental, and exergoenviroeconomic approaches: a comparative study. Sol Energy 2019;182:316–31.
[53] Yousef MS, Hassan H, Sekiguchi H. Energy, exergy, economic and enviroeconomic (4E) analyses of solar distillation system using different absorbing materials. Appl Therm Eng 2019;150:30–41.
[54] Sovacool BK. Valuing the greenhouse gas emissions from nuclear power: a critical survey. Energy Policy 2008;36:2950–63.
[55] Dwivedi VK, Tiwari GN. Thermal modeling and carbon credit earned of a double slope passive solar still. Desalin Water Treat 2010;13:400–10.
[56] Joshi P, Tiwari GN. Energy matrices, exergo-economic and enviro-economic analysis of an active single slope solar still integrated with a heat exchanger: a comparative study. Desalination 2018;443:85–98.
[57] Caliskan H. Energy, exergy, environmental, enviroeconomic, exergoenvironmental (EXEN) and exergoenviroeconomic (EXENEC) analyses of solar collectors. Renew Sustain Energy Rev 2017;69:488–92.
[58] Parsa SM, Rahbar A, Javadi Y D, Koleini MH, Afrand M, Amidpour M. Energy-matrices, exergy, economic, environmental, exergoeconomic, enviroeconomic, and heat transfer (6E/HT) analysis of two passive/active solar still water desalination nearly 4000m: altitude concept. J Cleaner Prod 2020;261:121243.
[59] Elbar ARA, Yousef MS, Hassan H. Energy, exergy, exergoeconomic and enviroeconomic (4E) evaluation of a new integration of solar still with photovoltaic panel. J Cleaner Prod 2019;233:665–80.
[60] Sahota L, Shyam GNT. Energy matrices, enviroeconomic and exergoeconomic analysis of passive double slope solar still with water based nanofluids. Desalination 2017;409:66–79.
[61] Kumar Singh A, Samsher. Material conscious energy matrix and enviro-economic analysis of passive ETC solar still. Mater Today: Proc 2021;38:1–5.